CHAPTER 4 FUZZY LOGIC CONTROL APPLICATION FOR TWIN ROTOR MIMO SYSTEM

Twin rotor multiple input multiple output system (TRMS) is a 2 degree of freedom system resembling a helicopter system, without elevation control. The reduced dof is due to the pivot point which is at the beam situated midway between tail-motor and the main-motor. Main rotor is driven by a DC motor and produces thrust to lift the beam resulting in a pitch angle movement. Similarly, the tail rotor driven by a DC motor produces thrust to rotate the beam in the left axis and the right axis resulting in yaw angle movement. Designing a controller for this kind of system is challenging due to their inherent instability, nonlinear dynamics and significant cross-coupling effects.

This chapter discusses the implementation of proposed controller for control of TRMS pitch and yaw angles. The proposed controller performance is compared to the performances obtained from real-time PID and fuzzy logic control based on following parameters:

- Transient response parameters: rise time, peak overshoot.
- Steady – state parameters: settling time, steady – state error.
- Performance indices.

4. 1 Problem formulation

From control engineering viewpoint TRMS demonstrates characteristics of a higher order nonlinear system along with significant cross-couplings. The control objective here is to control the “pitch” and “yaw” angle as per the given set-points while maintaining desired trajectory. Figure 4-1 illustrated the pitch and yaw angles associated to the main motor and tail motor respectively. The control philosophy for TRMS is as follows:

Pitch angle control: pitch angle is along the vertical axis (y-axis) and is controlled through the vertical thrust generated from “main motor”. Say for example if the “pitch angle” has to be reduced the “vertical thrust” should decrease hence voltage applied to the main motor is reduced in order to reduce the generated thrust and achieve the desired pitch angle.

Yaw angle control: yaw angle is along the horizontal axis and is controlled through the horizontal thrust generated from tail motor. Say for example if

"yaw angle" has to be decreased the "horizontal thrust" needs to be decreased hence the voltage applied to tail motor is decreased to decrease the generated thrust and achieve desired yaw angle.

4. 2 Mathematical modeling

Figure 4-1 depicts the forces acting on the rotors, and beam. The main rotor generates vertical thrust as a result produces torque for yaw movement. Similarly the tail motor generates horizontal thrust thereby producing torque for pitch movement.

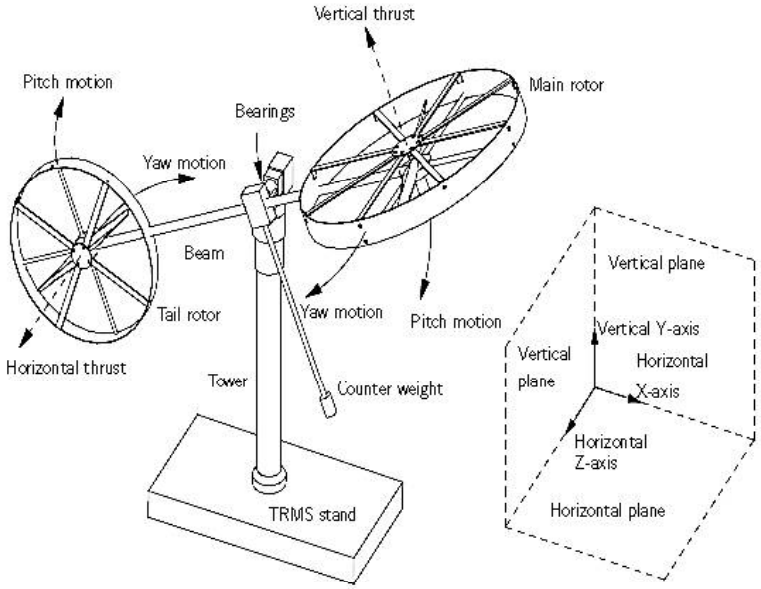

Figure 4-1 Forces acting on TRMS [97]

Since proposed FLC is independent of system model, the mathematical model is obtained for PID controller design. Due to non-linear and cross-coupled nature, the TRMS system is generally analysed in state space model. Standard dynamic equations for TRMS are [97]:

$$\frac{dx_1}{dt} = x_2$$

$$\frac{dx_2}{dt} = \frac{a_1}{I_1}x_5^2 + \frac{b_1}{I_1}x_5 - \frac{M_g}{I_1}sinx_1 + \frac{0.0326}{2I_1}\sin(2x_2)\,x_4^2 - \frac{B_{1\alpha v}}{I_1}x_2 - \frac{k_{gy}}{I_1}a_1\cos(x_1)\,x_4x_5^2 - \frac{k_{gy}}{I_1}b_1\cos(x_1)\,x_4x_5 \quad (4\text{-}1)$$

$$\frac{dx_3}{dt} = x_4$$

$$\frac{dx_4}{dt} = \frac{a_2}{I_2}x_6^2 + \frac{a_2}{I_2}x_6 - \frac{B_{1\alpha h}}{I_2}x_4 - \frac{k_c a_1}{I_2}1.75x_5^2 - \frac{1.75}{I_2}k_c b_1 x_5$$

$$\frac{dx_5}{dt} = -\frac{T_{10}}{T_{11}}x_5 + \frac{k_1}{T_{11}}u_v$$
$$\frac{dx_6}{dt} = -\frac{T_{20}}{T_{21}}x_6 + \frac{k_2}{T_{21}}u_h$$

The state variables are chosen as:

x_1 – Pitch angle
x_2 – Pitch angular velocity
x_3 – Yaw angle
x_4 – Yaw angle velocity
x_5 – Main motor momentum
x_6 – Tail motor momentum

Decoupled dynamics are illustrated as "vertical" and "horizontal" subsystems respectively [98].

$$x_v = [x_1\ x_2\ x_5\ x_7]$$
$$x_h = [x_3\ x_4\ x_6\ x_8] \quad (4\text{-}2)$$

The vertical system decoupled dynamics are:

$$\dot{x}_v = f_v(x_v, u_v)$$

Where, $f_v =$

$$\begin{bmatrix} \frac{a_1}{I_1}{x_5}^2 + \frac{b_1}{I_1}x_5 - \frac{M_g}{I_1}sinx_1 - \frac{B_{1\alpha_v}}{I_1}x_2 + \frac{0.0326}{2I_1}\sin(2x_1)\,x_4 \\ \frac{k_{gy}}{I_1}a_1\cos(x_1)\,x_4{x_5}^2 + \frac{k_{gy}}{I_1}b_1\cos(x_1)\,x_4x_5 \\ -\frac{T_{10}}{T_{11}}x_5 + \frac{k_1}{T_{11}}u_v \\ k_{iv}(r_v - x_1) \end{bmatrix} \quad (4\text{-}3)$$

The horizontal system decoupled dynamics are:

$$\dot{x}_h = f_h(x_h, u_h)$$

Where, $f_h =$

$$\begin{bmatrix} \frac{a_2}{I_2}{x_6}^2 + \frac{b_2}{I_2}x_6 - \frac{B_{1\alpha_h}}{I_2}x_4 - \frac{k_c a_1}{I_2}1.75{x_5}^2 - \frac{1.75}{I_2}k_c b_1 x_5 \\ -\frac{T_{20}}{T_{21}}x_6 + \frac{k_2}{T_{21}}u_h \\ k_{ih}(r_h - x_3) \end{bmatrix} \quad (4\text{-}4)$$

here $k_{ih}$and $k_{iv}$are the internal gains. The parameters of hardware model used are described in Table 4-1.

Table 4-1 Parameters of the physical model used

Symbol	Description	Value
l_1	Moment of inertia for vertical rotor	0.068 kgm^2
l_2	Moment of inertia for tail rotor	0.02 kgm^2
a_1	Static characteristic	0.0135 N/A
b_1	Static characteristic	0.0294 m
a_2	Static characteristic	0.02 m
b_2	Static characteristic	0.09 m
M_g	Gravity momentum	0.32 Nm
$B_{1\alpha v}$	Friction momentum function	0.006 Nms/rad
$B_{1\alpha h}$	Friction momentum function	0.1 Nms/rad
k_{gy}	Gyroscopic momentum	0.0155 s/rad
k_1	Main rotor gain	1.1
k_2	Tail rotor gain	0.8
T_{11}	Main rotor denominator	1.1
T_{10}	Main rotor denominator	1
T_{21}	Tail rotor denominator	1
T_{20}	Tail rotor denominator	1
T_p	Cross reaction momentum parameter	2
T_o	Cross reaction momentum parameter	3.5
k_c	Cross reaction momentum gain	-0.2

The hardware utilized for experimental purpose is developed by Feedback Instruments Ltd. depicted in Figure 4-2 (a) and Figure 4-2 (b) depicts the block diagram and connection of various components with PC and DAQ card.

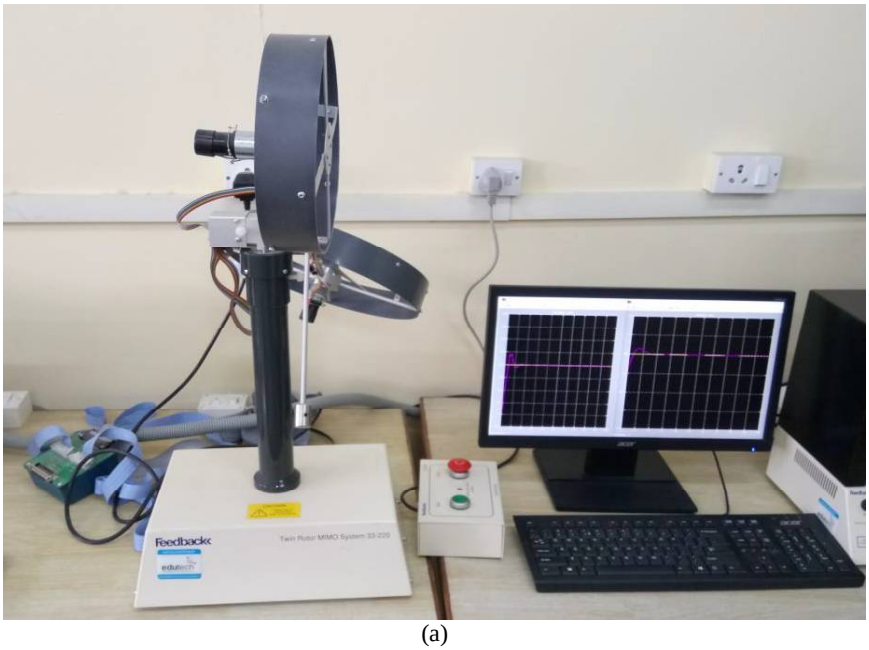

(a)

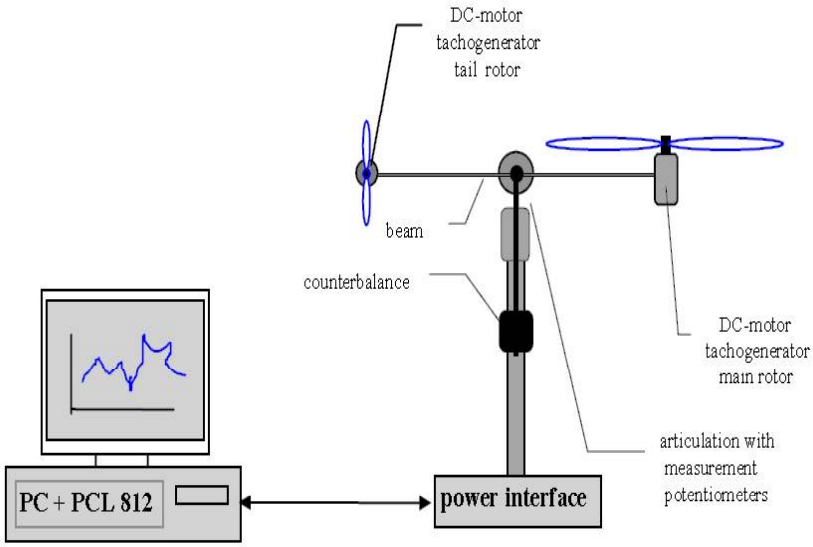

(b)

Figure 4-2 (a) Real-time DPCS system available in Control theory and simulation lab, UPES (b) Connection block diagram for TRMS setup [97]

The DAQ card (power interface module) acts as a real-time interface device between the analog system and the digital computer. The tail rotor and the main rotor are attached with tachogenerators which measure their angular positions. The DAQ card converts the analog signal form tachogenerators are to digital signals, which is then transferred to computer. Control signal generated form PC (via Matlab-Simulink™) is converted into analog form and transferred to the tail and main motors using the power interface module.

4. 3 Fuzzy logic control

As stated in section 3. 3 FLC designed is independent of mathematical model of system dynamics however; the tuning of PID controller is based on system dynamics. Therefore FLC is designed as a controller independent by treating the TRMS as a black-box system overlooking the system model and using the expert knowledge. PID controller is designed around linear decoupled model of the system under study.

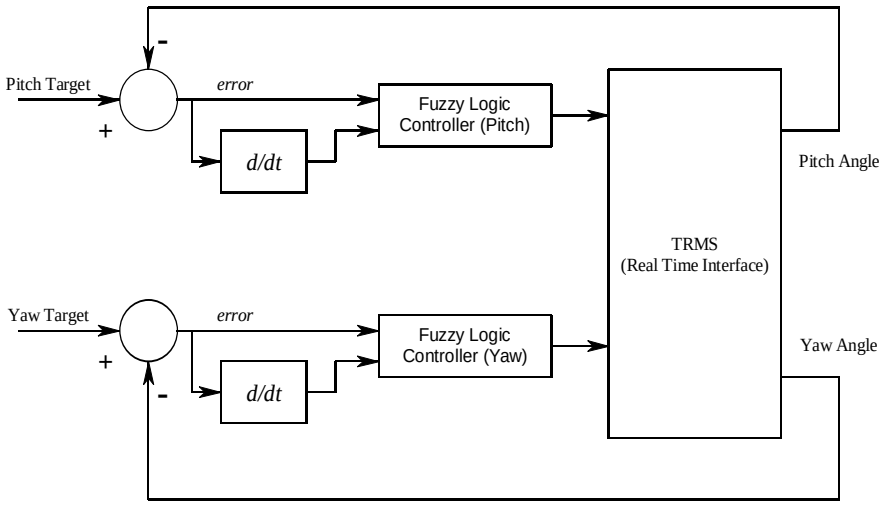

Figure 4-3 Fuzzy logic control for TRMS

The fuzzy logic control architecture for TRMS system is depicted in Figure 4-3. Here, two separate PD type fuzzy logic controllers are used to control the "pitch angle" and "yaw angle" respectively. The inherent advantage of FLC is the competency to handle non-linear systems, since FLC design is independent of the system model, therefore the control system designer can overlook the system dynamics and cross-coupling efects. The initial FS designed for TRMS fuzzy logic control are illustrated in Figure 4-4. The sets are considered equally distributed around the error. The sets are designed according to the procedure discussed in section 2. 4; where the sets are nomenclated named in according to their relative position with error.

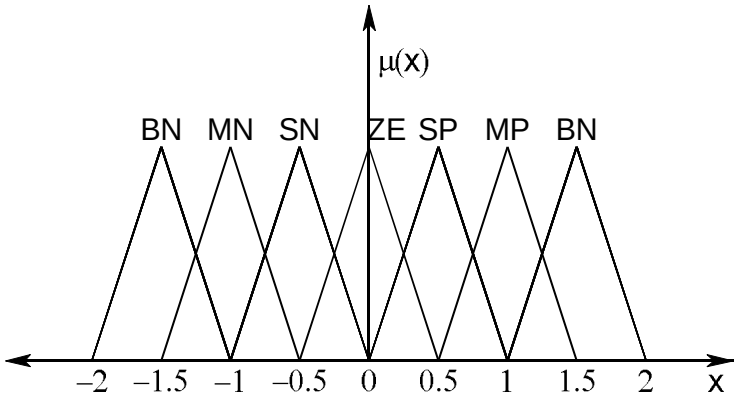

Figure 4-4 FS for pitch angle and yaw angle error

FS for "$\dot{e}$ – rate of change of error" & "c – control force" are designed using same principle. The range for these sets is:

$\dot{e}_{pitch} = [-3.21, 3.2]$ $\dot{e}_{yaw} = [-2.4, 2.4]$ $c = [-5, 5]$

The fuzzy rule base employed is derived from system control philosophy illustrated in section 4. 1. Since the control logic for both the pitch angle and the yaw angle are same the same rule base is employed for pitch and yaw controllers. The difference lies in the input variables. For pitch angle controller the input is the error observed in pitch angle. For yaw angle controller the input is the error observed in yaw. The rule base for error, rate of change of error vs control force is summarized in Table 4-2

Table 4-2 Rule base for pitch/yaw angle error, rate of change of error and Control signal

Control force		Rate of change of error $(\dot{e})$						
		BN	MN	SN	ZE	SP	MP	BP
Error in angle (e)	BN	BN	BN	BN	BN	BN	MN	SN
	MN	BN	BN	BN	BN	SN	ZE	SP
	SN	BN	BN	BN	SN	ZE	SP	MP
	ZE	BN	MN	SN	ZE	SP	MP	BP
	SP	MN	SN	ZE	SP	BP	BP	BP
	MP	SN	ZE	SP	BP	BP	BP	BP
	BP	SP	MP	BP	BP	BP	BP	BP

For example a detailed rule for pitch angle control can is depicted as:

If e is "small negative" and $\dot{e}$ is "zero" than c should be "small negative".

A "small negative" error indicates that the pitch angle is more than the desired angle, and "zero" rate of change in angle means that the pitch angle is not changing. This clearly indicates that the vertical thrust needs to be reduced in order to achieve the desired pitch angle. Hence the main motor control voltage is decreased from the existing value to achieve the "desired" pitch angle.

4. 4 Optimized fuzzy logic control

For optimization process the displaced FSs are employed to obtain optimized FS. Standard deviation (σ) calculated for pitch angle data and yaw angle data are:

SD for Pitch angle data:	SD for Yaw angle data:
error = 0.1	error = 0.2
Rate of change of error = 0.37	Rate of change of error = 0.28
Control force = 0.23	Control force = 0.14

The optimization objective function is written as:

$$\text{Maximize } H(A) = \int_a^b f\left(\frac{x-a}{b-a}\right)dx + \int_b^c f\left(\frac{x-c}{b-c}\right)dx \quad (4\text{-}5)$$

Subject to maximum $H(\mu) = \sum_{i=1}^{n} H(\mu_i)$

Maximize

$$H(\mu_{z^*}) = -\left[\int_{-\varepsilon\mp\sigma}^{0}\left(\frac{x+\varepsilon\mp\sigma}{\varepsilon\mp\sigma}\right) ln\left(\frac{x+\varepsilon\mp\sigma}{\varepsilon\mp\sigma}\right) dx + \int_{-\varepsilon\mp\sigma}^{0}\left(-\frac{x}{\varepsilon\mp\varepsilon}\right) ln\left(-\frac{x}{\varepsilon\mp\varepsilon}\right) dx\right] - \left[\int_{0}^{\varepsilon\pm\sigma}\left(\frac{\varepsilon\pm\sigma-x}{\varepsilon\pm\sigma}\right) ln\left(\frac{\varepsilon\pm\sigma-x}{\varepsilon\pm\sigma}\right) dx + \int_{0}^{\varepsilon\pm\sigma}\left(\frac{x}{\varepsilon\pm\sigma}\right) ln\left(\frac{x}{\varepsilon\pm\sigma}\right) dx\right] \quad (4\text{-}6)$$

Subject to maximum $H(\mu) = \sum_{i=1}^{n} H(\mu_i)$

An example of the displaced set can be seen in Figure 4-5 where FS "Zero" for error in pitch angle is shown after displacement.

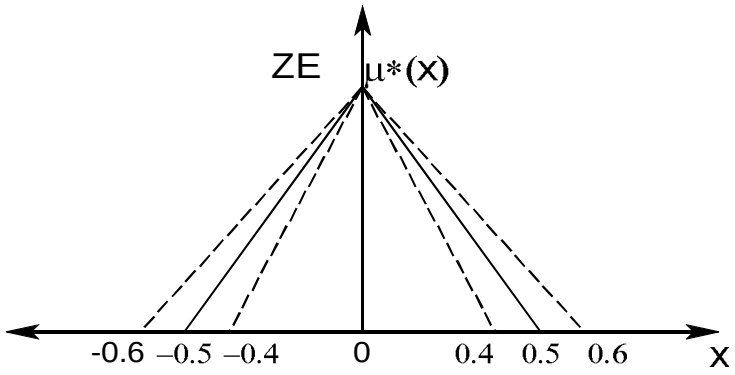

Figure 4-5 FS for error in pendulum angular position

4. 5 Simulation model and real-time experiment results

Figure 4-6 depicts the simulation model for TRMS and model parameters are illustrated in Figure 4-7.

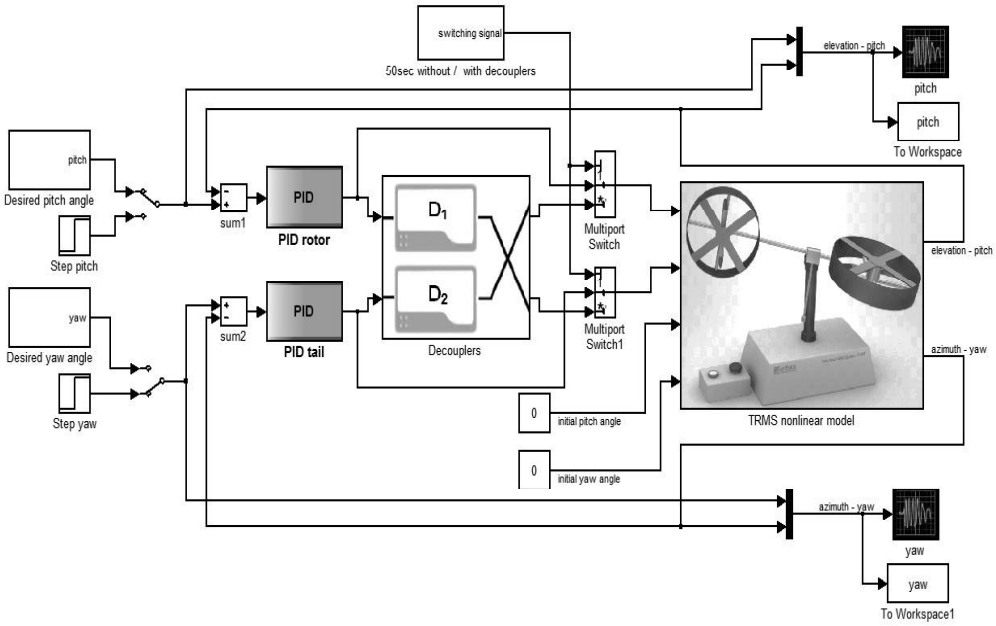

Figure 4-6 Simulation model for twin rotor MIMO system

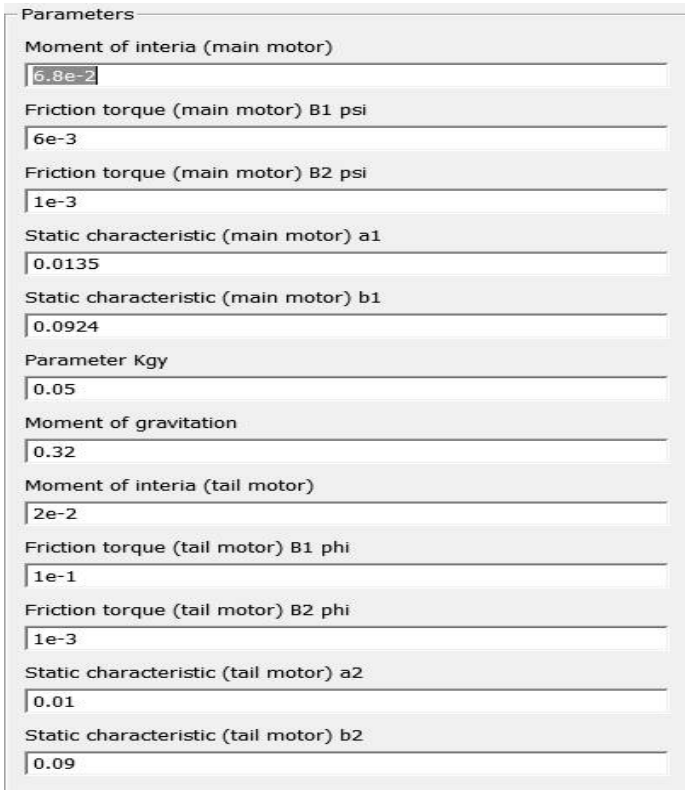

Figure 4-7 Parameters for simulation model

Here, the system simulation objective is: to maintain a desired system trajectory specified. The desired trajectory is fed to the controllers along with the pitch angle & yaw angle measurements. Depending on the error obtained PID controllers generate the control voltage required to vary vertical & horizontal thrusts respectively.

The results depicted here are obtained from real-time hardware model depicted in Figure 4-2 (a). Since the TRMS is a cross-coupled system the first step to design a PID controller is the decoupled model design, therefore PID simulation model depicted here consist of decouplers. For trajectory control of TRMS system 2 separate controllers are designed for "pitch angle" and "yaw angle" respectively. The PID gains are obtained using the optimized Zeigler-Nichols (ZN) tuning method. Here the PID gains are initially obtained using ZN tuning and are then optimized for minimum error-indices [97]. This is obtained from simulation model of TRMS system. Due to cross-coupling designing a PID controller for TRMS is a challenging task since performance of PID controller is based on decoupled system dynamics. If the decoupling

blocks are not premeditated accurately it leads to inefficient and sometimes unstable PID controller.

The performance for various controllers is evaluated using common system trajectories:

1. Step input as change in desired trajectory.
2. Series of step changes of various magnitudes in desired trajectory.
3. Sinusoidal input as change in desired trajectory.

4. 5. 1 Real-time PID control

The results for optimized controller are compared with benchmark PID controller. PID controller is tuned for linear decoupled model as discussed above. The optimized PID gains are:

Pitch Controller	$K_P = 3$	$K_I = 8$	$K_D = 10$
Yaw Controller	$K_P = 2$	$K_I = 0.5$	$K_D = 5$

Real-time PID controller response to a step change in pitch and yaw angle are given in Figure 4-8. Here, the set-point for pitch angle is changed by a step of 0.4 radians; and the yaw angle set-point is varied by a step change of 0.5 radians as illustrated in Figure 4-8 (a) and Figure 4-8 (b) respectively. The set-point tracking for pitch and yaw angle results exhibit zero steady-state error ($e_{ss} = 0$).

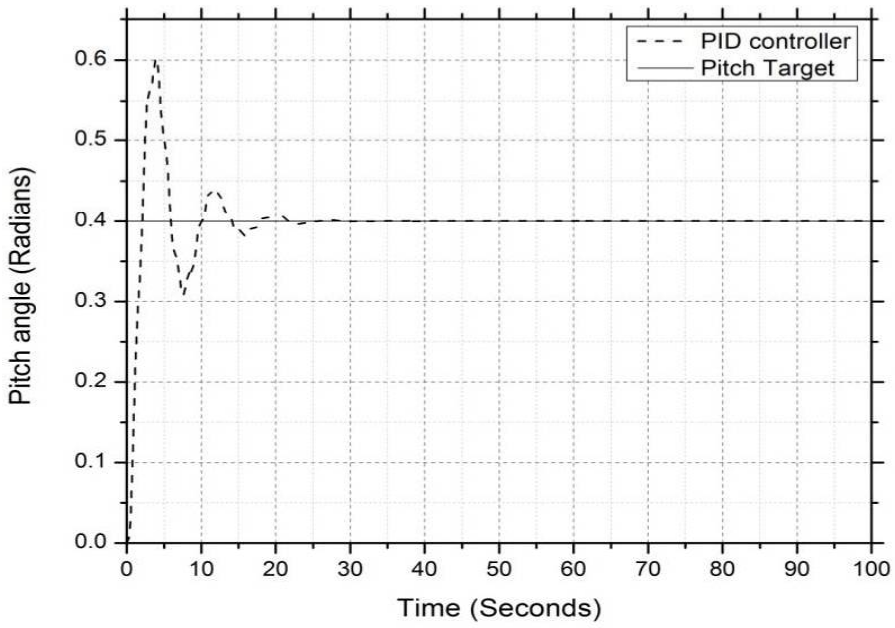

(a)

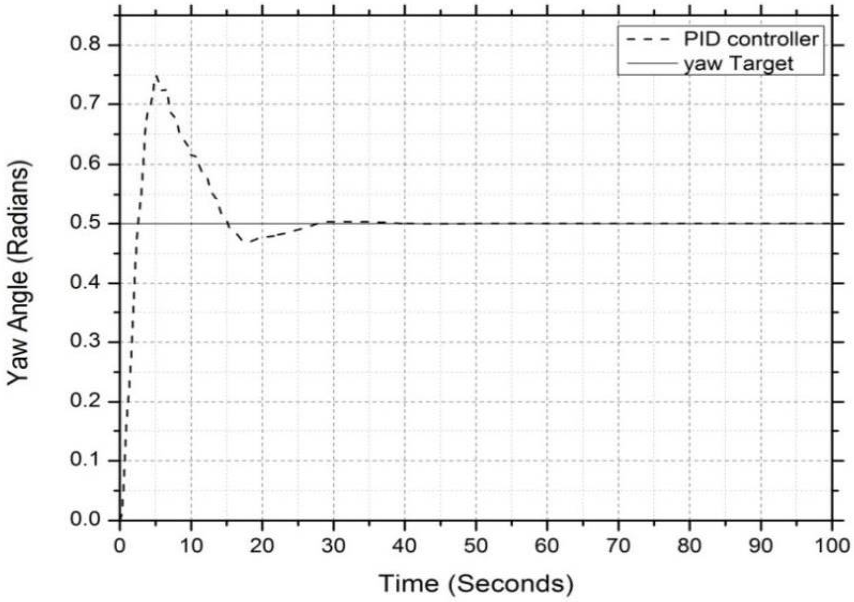

(b)

Figure 4-8 PID controller response for (a) 0.4 radian change pitch angle, (b) 0.5 radian change in yaw angle

The pitch angle and yaw angle response exhibits an overshoot of 50 %, this can be reduced by varying PID gain(s) for lower overshoot, but will result in a sluggish system response, due to which "rise time" and "settling time" increases. Another effect is the loss of generality for set-point tracking which is evident from Figure 4-9 where, set-point is changing rapidly. Hence the parameters for PID are chosen to obtain a fast set-point tracking. Table 4-3 summarizes the performance indices, transient, and steady state response parameters for PID controller response.

Table 4-3 Performance indices for PID controller with unit step set-point change

	Values	
Parameter	Pitch angle	Yaw angle
Peak overshoot (M_p)	50%	50 %
Rise time (seconds)	2	3
Settling time (seconds)	23	27
ISE	0.2295	0.5246
ITSE	0.4953	2.059
IAE	1.318	2.537
ITAE	6.356	17.87

The set-point for pitch angle is now changed to a combination of step changes of varying amplitude as illustrated in Figure 4-9(a). Advantage of having faster rise time and settling time is apparent from the "dynamically changing" pitch angel set-point depicted in Figure 4-9(a).

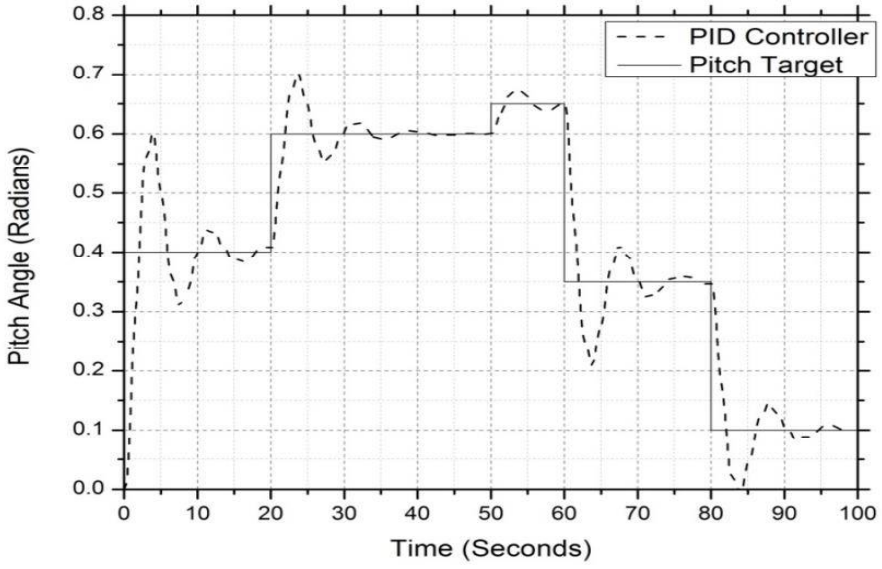

(a)

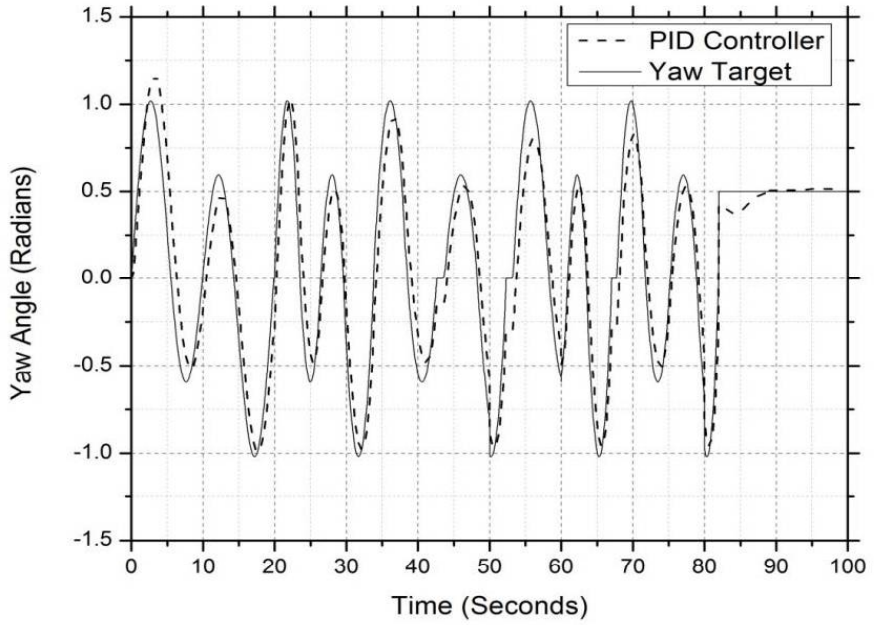

(b)

Figure 4-9 PID control response for periodic change in set – point of (a) Pitch angle (b) Yaw angle

The steady-state error is zero ($e_{ss} = 0$) despite of the rapid changes in the set-point of pitch angle. Similarly the yaw angle response for PID controller is illustrated in Figure 4-9(b); here the set-point is a sinusoidal signal converging to a constant step. The "error indices" for PID controller response are illustrated in Table 4-4.

Table 4-4 Performance indices for PID controller with random set-point change

Error indices	ISE	ITSE	IAE	ITAE
Pitch Control	0.4771	15.05	3.762	149.1
Yaw Control	3.781	171.1	16.85	806.9

4. 6 Real-time fuzzy logic control

The system performance is now evaluated for real-time FLC, depicted in Figure 4-3. PID controllers are replaced by FLC. Figure 4-10 depicts the real-time system response for FLC. Figure 4-10(a) depicts the pitch angle response for a step change in set-point by 0.5 radians. Figure 4-10(b) depicts the yaw angle response for a step change in set-point by 0.4 radians. Real-time response indicates a zero steady state error $(e_{ss} = 0)$ for FLC based "pitch angle" and "yaw angle" control same as PID controller. However transient parameters are now improved. The peak overshoot for pitch angle control response through FLC is 42% indicating a reduction of 8% over PID controller. Similarly, the peak overshoot for yaw angle control response through FLC is 30%, indicating a reduction of 20% as compared with PID controller.

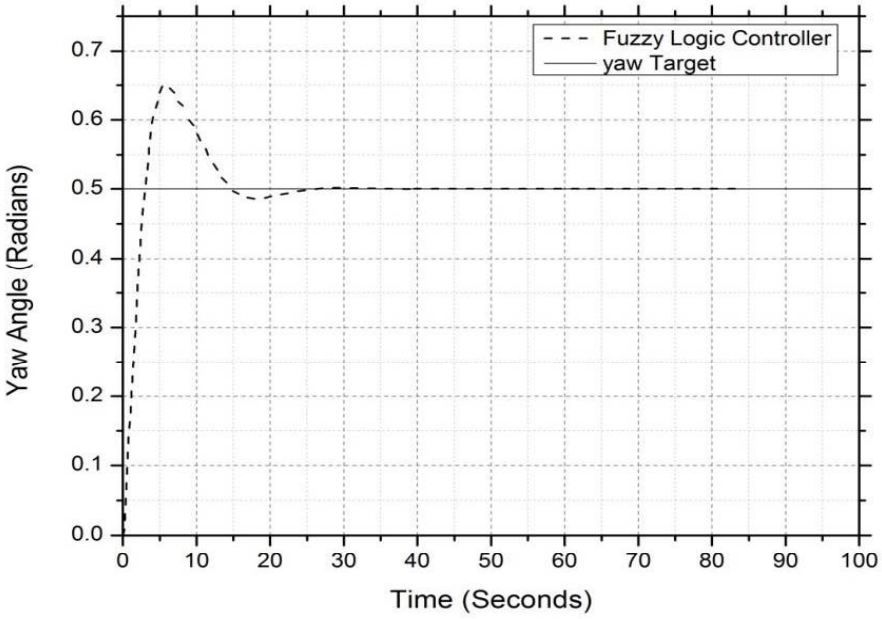

(a)

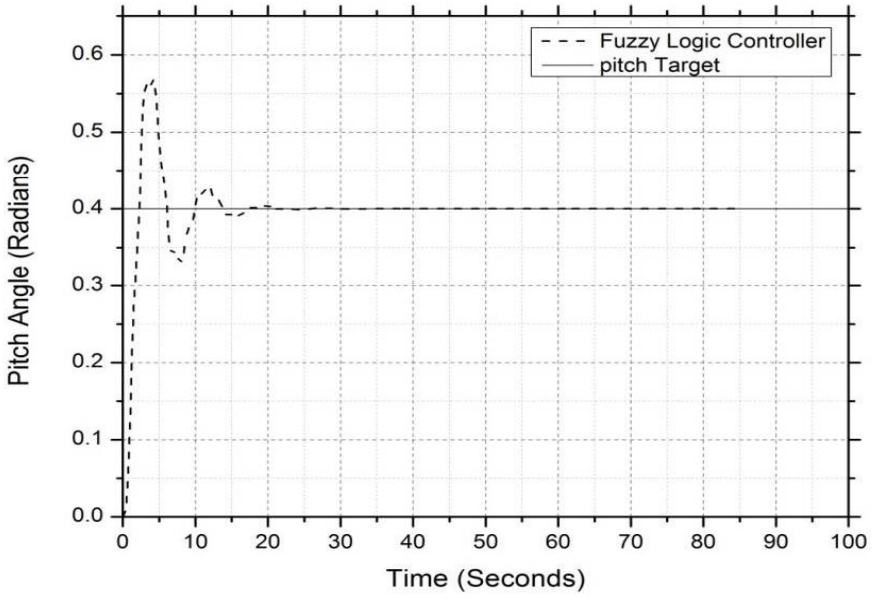

(b)

Figure 4-10 FLC response (a) step change of 0.4 radians for Pitch angle (b) step change of 0.5 radians for Yaw angle

Table 4-3 summarizes the performance parameters for FLC. A direct comparison of these parameters with PID controller parameters indicates that FLC is better than PID controller. An important observation is: peak overshoot for PID controller can be reduced to match with FLC, but this result in a sluggish system hence affects the transient and steady-state parameters. However FLC not just indicates an improvement in transient parameters but also an improvement in steady-state parameters as well.

Table 4.3 Performance indices for real-time FLC with step change in set-point.

	Values	
Parameter	Pitch angle	Yaw angle
Peak overshoot (M_p)	42 %	30%
Rise time (seconds)	1.5	2
Settling time (seconds)	15	22
ISE	0.2254	0.3579
ITSE	0.4269	1.05
IAE	1.245	1.888
ITAE	5.512	11.57

The set-point for pitch angle is changed to a combination of varying amplitude step changes illustrated in Figure 4-11(a). Similarly, set-point for yaw angle is given as a sinusoidal signal converging to a constant step as illustrated in Figure 4-11(b). These results are obtained for set-point tracking by FLC and results indicate a zero steady state error $(e_{ss} = 0)$ for both "pitch angle" & "yaw angle".

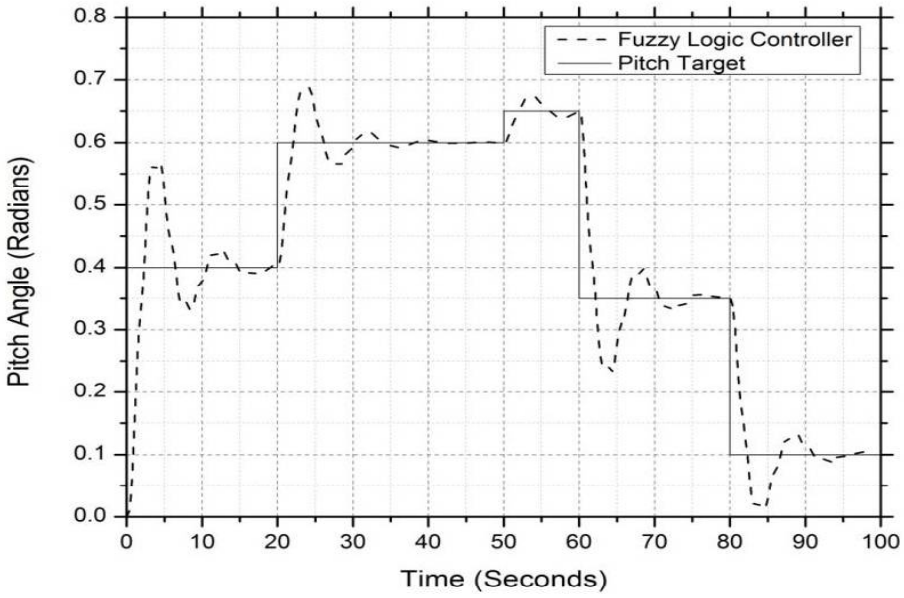

(a)

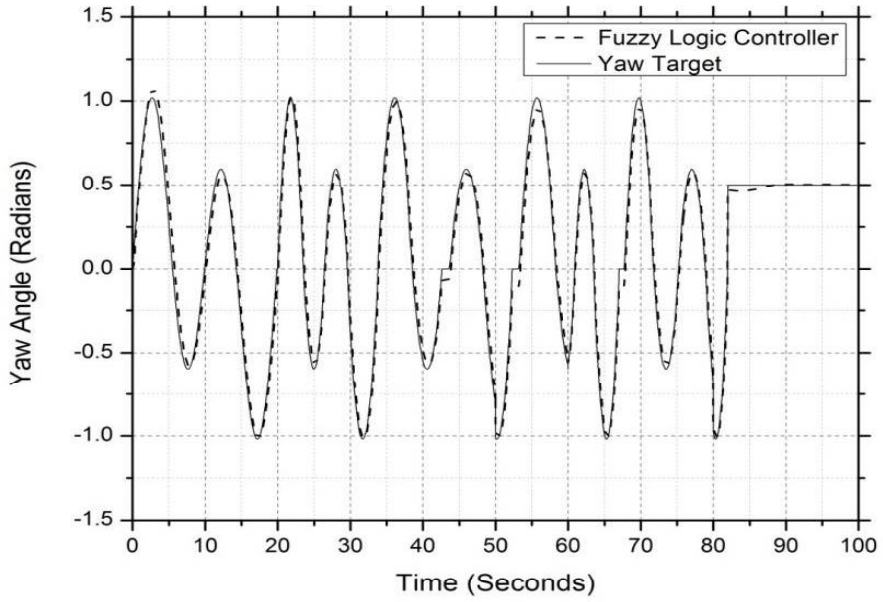

(b)

Figure 4-11 FLC response for dynamically changing (a) Pitch angle set – point , (b) Yaw angle set – point

Table 4-5 Performance indices for FLC with dynamically changing set-point

Error indices	ISE	ITSE	IAE	ITAE
Pitch Control	0.4735	14.7	3.644	141
Yaw Control	0.4844	21.71	6.069	289

The system now exhibits lesser overshoots due to which settling time is now decreased since steady state is attained early. The response now exhibits lower oscillations and “error indices” are given in Table 4-5.

4. 7 Real-time optimized fuzzy logic control

After optimization predefined sets of FLC are now replaced by "optimized" sets. The performance for optimized FLC is analyzed for same set-points as given for PID and FLC.

Figure 4-12(a) depicts the response for optimized FLC to 0.4 radians change in pitch angle set-point. The peak overshoot for pitch angle is now reduced to 20% which is a reduction of about 30% when compared to PID controller. Figure 4-12 (b) depicts the response for optimized FLC to 0.5 radians change in yaw angle set-point. The overshoot for yaw angle is reduced to 29% which is a reduction of 21% when compared to PID controller. Table 4-6 summarizes the performance indices for optimized FLC indicated in Figure 4-12.

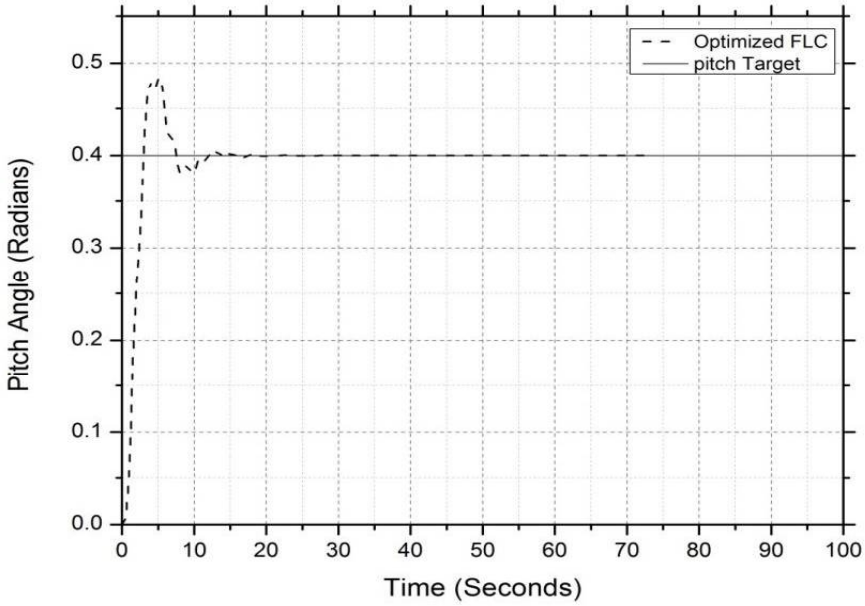

(a)

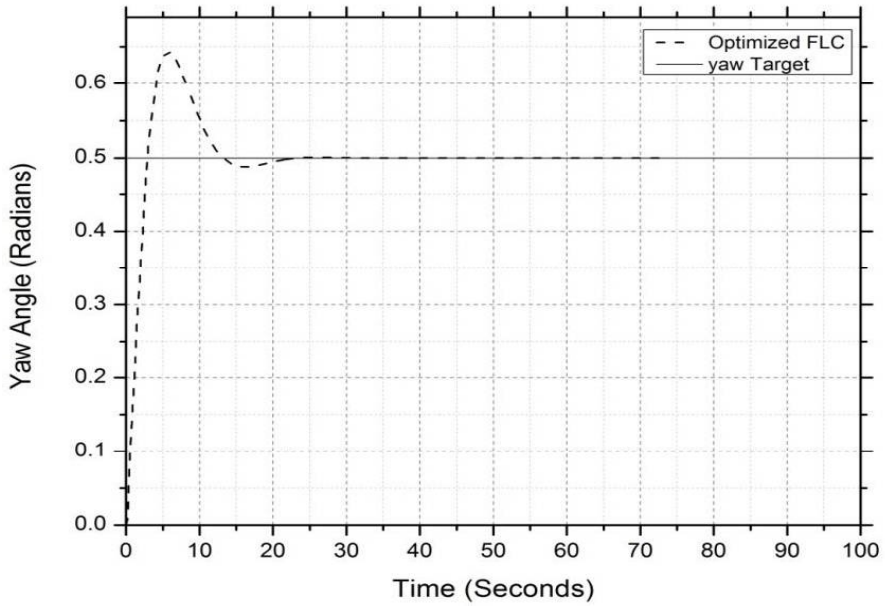

(b)

Figure 4-12 Optimized FLC response (a) step change of 0.4 radians for Pitch angle (b) step change of 0.5 radians for Yaw angle

Table 4-6 Performance indices for Optimized Fuzzy Logic Controller with unit step set-point change

	Values	
Parameter	Pitch angle	Yaw angle
Peak overshoot (M_p)	20%	29%
Rise time (seconds)	1.5	2
Settling time (seconds)	11	18
ISE	0.2442	0.3515
ITSE	0.3042	1.004
IAE	1.121	1.832
ITAE	3.642	10.88

The step changes of set-point are changed to dynamically changing set-point. Figure 4-13(a) depicts the response for optimized FLC to dynamic change in pitch angle set-point. Figure 4-13(b) depicts the response for optimized FLC to yaw angle set-point. Optimized FLC exhibits faster transients; thereby resulting in a lower settling time with minimal overshoot when compared with PID or FLC.

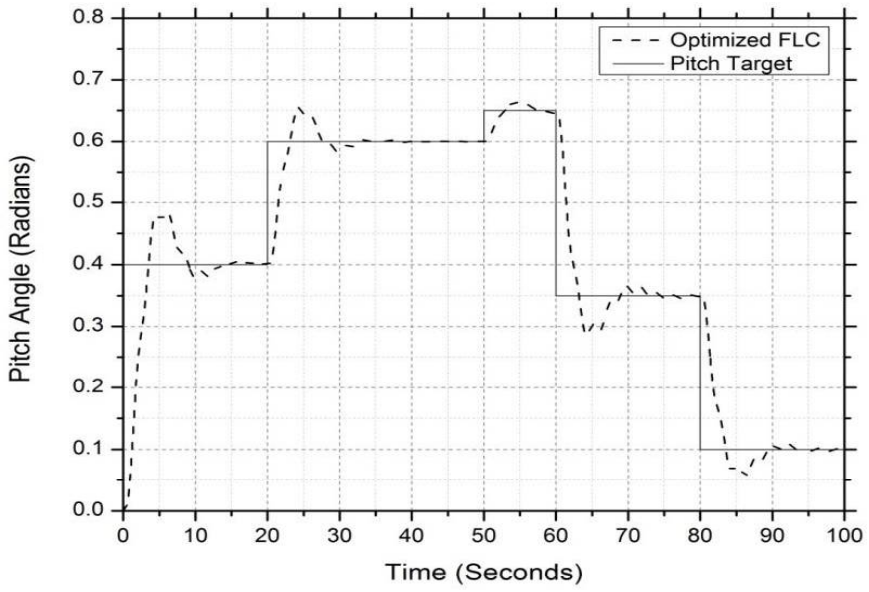

(a)

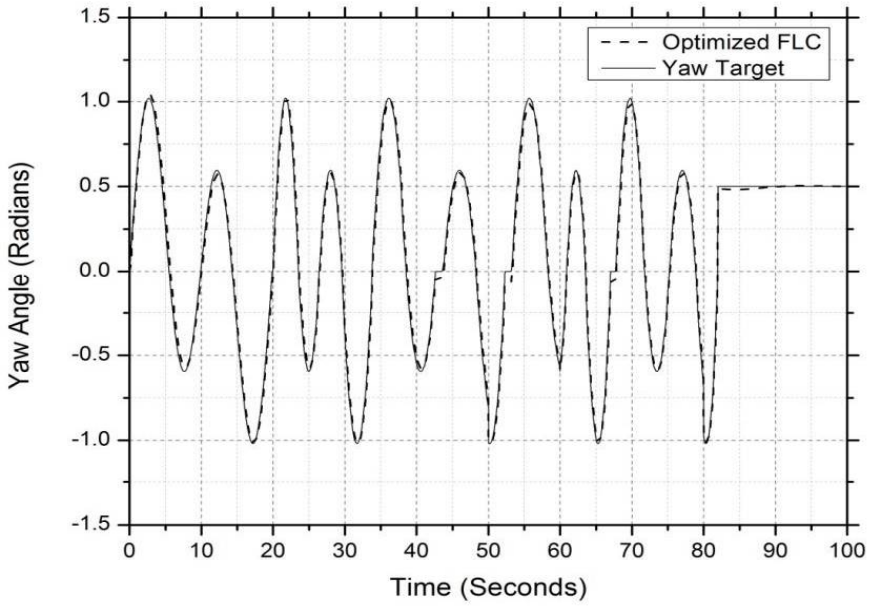

(b)

Figure 4-13 Optimized FLC response for dynamically changing (a) Pitch angle set-point (b) Yaw angle set-point

Table 4-7 summarizes the performance indices for optimized FLC indicated in Figure 4-13. A direct comparison of these parameters with PID controller parameters indicates that optimized FLC is better than PID controller. Both transient & steady-state parameters observe an improvement as compared with PID or FLC. Due to this error indices are also significantly reduced.

Table 4-7 Performance indices for FLC with dynamically changing set-point

Error indices	ISE	ITSE	IAE	ITAE
Pitch Control	0.5115	15.62	3.486	134.9
Yaw Control	0.1794	7.994	3.698	175.9

4. 8 Comparative analysis

Figure 4-14 depicts one-to-one comparison for the responses obtained from PID controller, FLC and optimized FLC. Figure 4-14(a) illustrates the responses for a step change (0.4 radians) in pitch angle set-point. Figure 4-14(b) illustrates the responses for a step change (0.5 radians) in yaw angle set-point. Results clearly indicate an improvement in transient and steady-state parameters for optimized FLC as it exhibits lower overshoot and lower settling time.

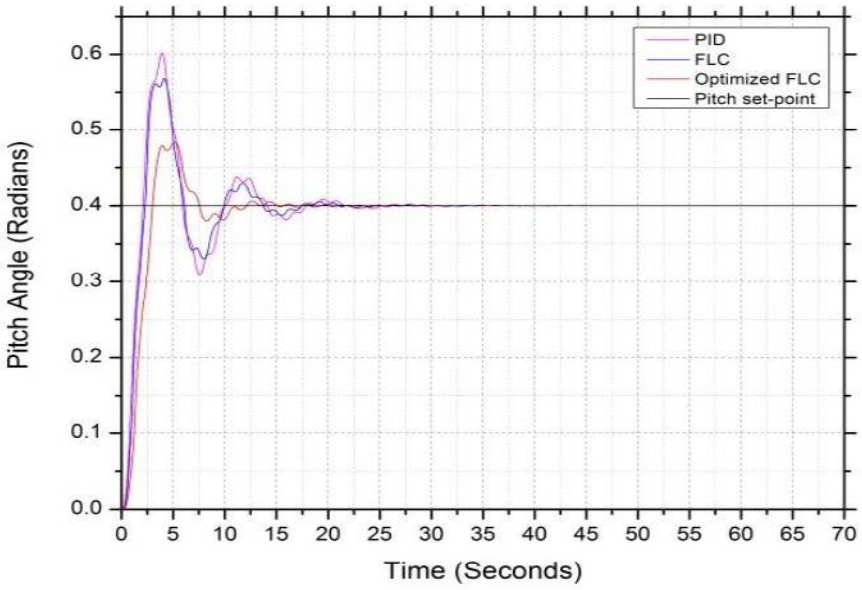

(a)

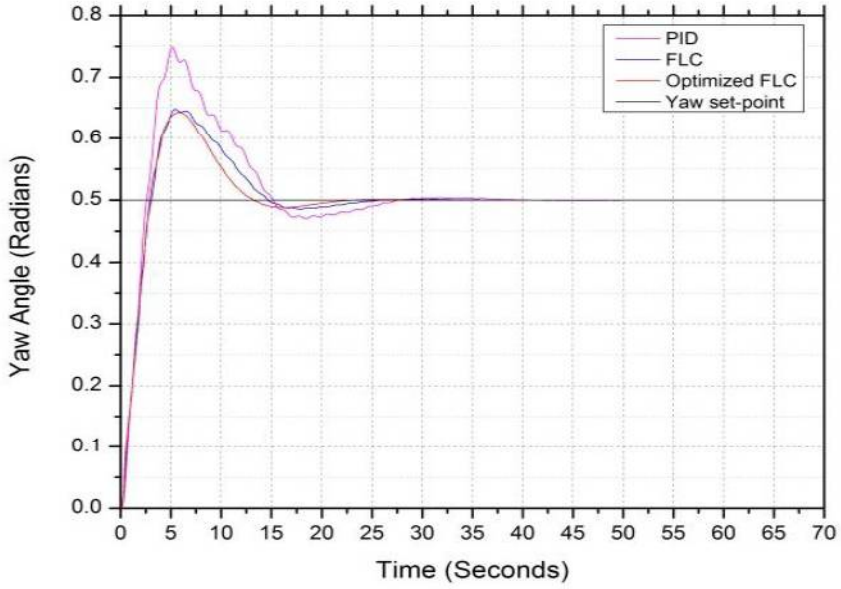

(b)

Figure 4-14 (a) Pitch angle response for a step change of 0.4 radians (b) Yaw angle response for a step change of 0.5 radians

Transient, steady-state parameters, error indices for PID, FLC, and optimized FLC are summarized in Table 4-8. The overshoot for pitch angle set-point tracking is reduced to 20% for optimized FLC, as compared with 42% for FLC and 50% for PID controller. The overshoot for yaw angle set-point tracking is reduced to 29% for optimized FLC, as compared with 30% for FLC and 50% for PID controller. Error indices for optimized FLC exhibit lower values as compared with FLC or PID controller.

Table 4-8 Performance indices comparison for PID, FLC and optimized FLC for step change in set point

Pitch Angle			
Parameter	PID	FLC	Optimized FLC
Peak overshoot	50%	42 %	20%
Rise time	2 s	1.5 s	1.5 s
Settling time	23 s	15 s	11 s
ISE	0.2442	0.2295	0.2254
ITSE	0.4953	0.4269	0.3042
IAE	1.318	1.245	1.121
ITAE	6.356	5.512	3.642

Yaw Angle			
Parameter	PID	FLC	Optimized FLC
Peak overshoot	50 %	30%	29%
Rise time	3 s	2 s	2 s
Settling time	27 s	22 s	18 s
ISE	0.5246	0.3579	0.3515
ITSE	2.059	1.05	1.004
IAE	2.537	1.888	1.832
ITAE	17.87	11.57	10.88

The step changes of set-point are now replaced with dynamically changing set-point. The set-point for pitch angle is a combination of step changes, and set-point for yaw angle is a sinusoidal signal converging to step. Pitch angle & yaw angle responses for PID, FLC and optimized FLC are depicted in Figure 4-15. Figure 4-15(a) illustrates the comparison for set-point tracking of pitch angle for PID, FLC and optimized FLC respectively. The response for optimized FLC settles quite well before the step changes are introduced due to lower “settling time”. Figure 4-15(b) illustrates the comparison for set-point tracking of yaw angle for PID, FLC and optimized FLC.

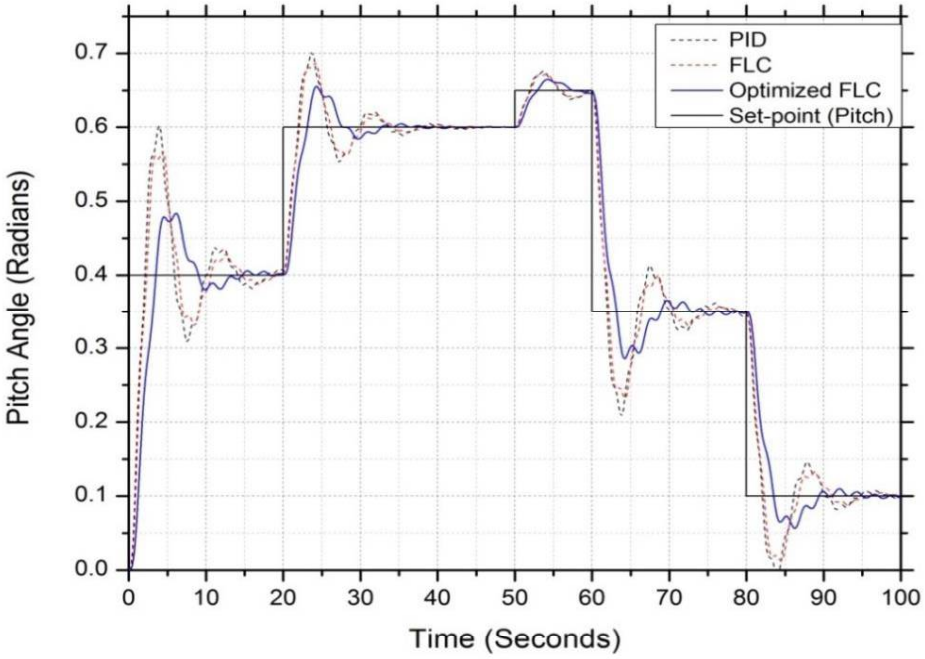

(a)

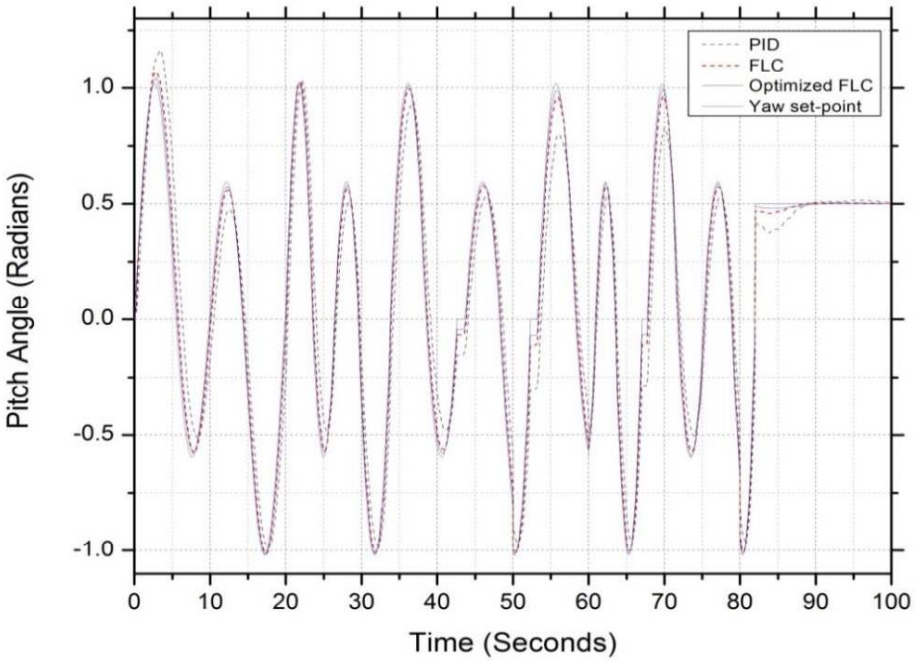

(b)

Figure 4-15 (a) Pitch angle response (b) Yaw angle response

Performance parameters for PID control, fuzzy logic control, and proposed optimized fuzzy logic control are compared in Table 4-9. These parameters evaluated from real-time system response validate superior performance for optimized FLC when compared to PID control, or fuzzy logic control (non-optimized).

Table 4-9 Comparison of performance indices for PID, FLC and optimized FLC for dynamically changing pitch and yaw angle set-points

	Pitch Angle			
Error indices	ISE	ITSE	IAE	ITAE
PID	0.4771	15.05	3.762	149.1
FLC	0.4735	14.7	3.644	141
Optimized FLC	0.5115	15.62	3.486	134.9

	Yaw angle			
Error indices	ISE	ITSE	IAE	ITAE
PID	3.781	171.1	16.85	806.9
FLC	0.4844	21.71	6.069	289
Optimized FLC	0.1794	7.994	3.698	175.9

4. 8. 1 Comparison of proposed controller with referenced work

The Performance obtained from real-time implementation of proposed controller is compared with some reference controllers which employ FLC for TRMS control.

Jahed [38] employed adaptive FLC for pitch and yaw angle control for TRMS. The architecture utilized in Jahed's FLC is same as the proposed controller, where two independent FLCs for pitch and yaw angles control are deployed. Jahed's fuzzy controller employed Gaussian membership function. Gradient descent learning method is based on minimization of:

$$E(k) = \frac{1}{2}\left[f\left(x(k)\right) - y(k)\right]^2 \tag{4-7}$$

here $f(x(k))$ is: output for FLC, and $y(k)$ is: actual output for TRMS system. Equation (4-7) depicts the learning rule, and is written as following for horizontal and vertical axes:

$$E_h(k) = \frac{1}{2}\left[r_h^d(k) - y_h(k)\right]^2 \tag{4-8}$$

$$E_v(k) = \frac{1}{2}\left[r_v^d(k) - y_v(k)\right]^2 \tag{4-9}$$

Here $r_h^d(k)$and $r_v^d(k)$are: set-point for yaw angle (horizontal-axis) and pitch angle (vertical-axis) respectively.

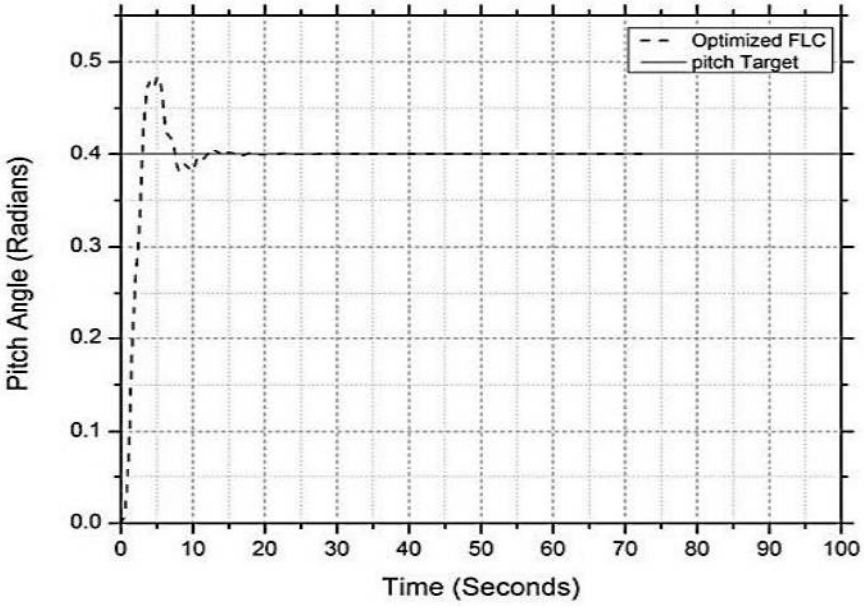

(a)

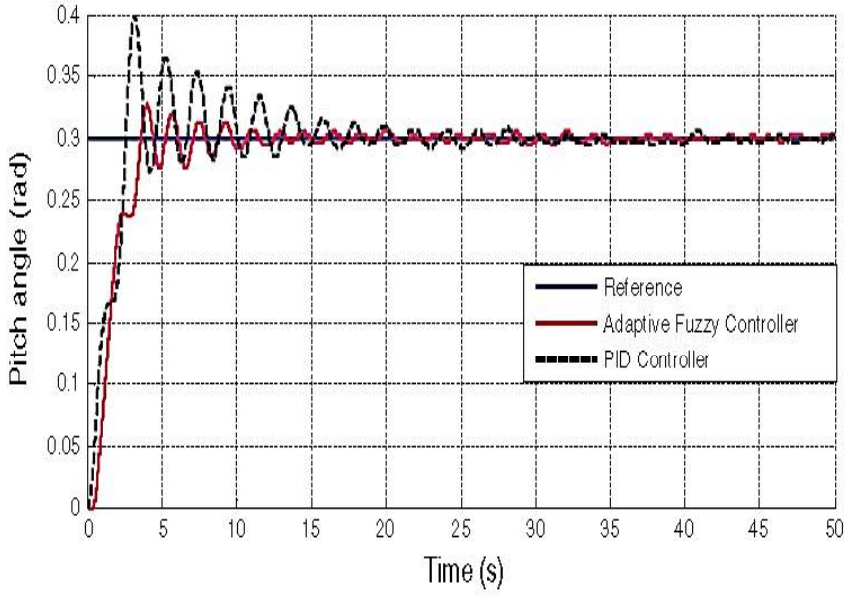

(b)

Figure 4-16 Pitch angle set-point tacking response (a) proposed controller (b) reference controller **[38]**

Figure 4-16 depicts comparison for pitch angle set-point tracking for (a) proposed controller with (b) Jahed's gradient descent learning method based adaptive FLC. Similarly Figure 4-17 depicts the comparison of set point tracking for yaw angle.

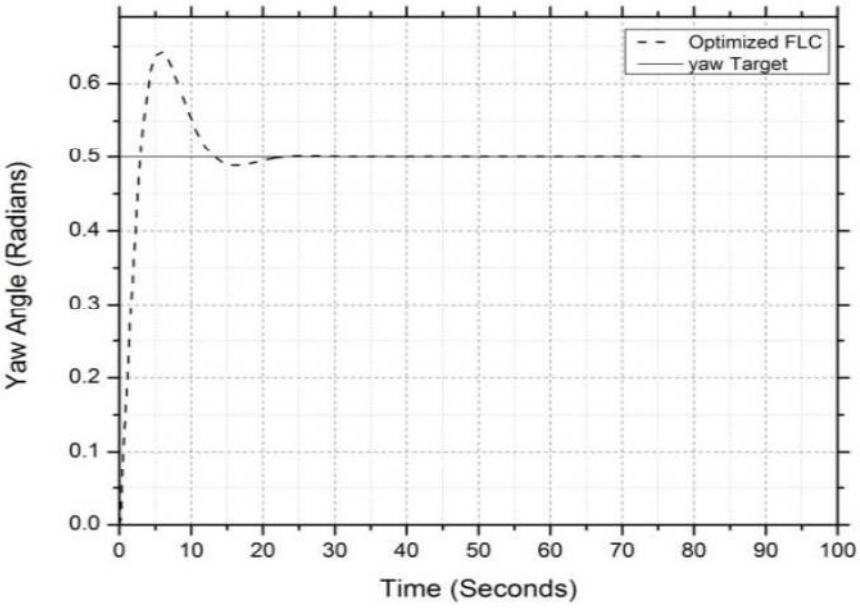

(a)

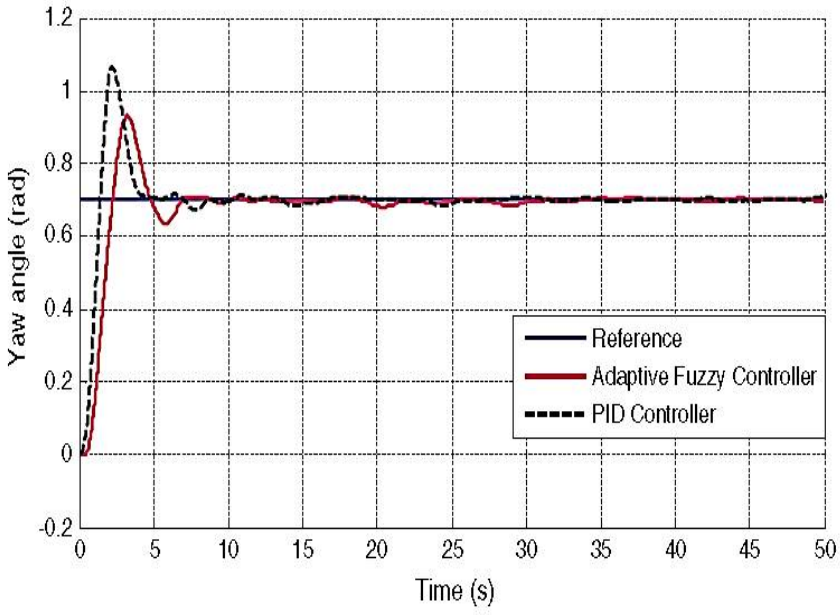

(b)

Figure 4-17 Yaw angle set-point tacking response (a) proposed controller (b) reference controller [38]

Table 4-10 illustrates the comparison between pitch angle response for proposed controller and Jahed's adaptive FLC in terms of: transient parameters, steady-state parameters. Table 4-11 illustrates the comparison between yaw angle response for proposed controller and Jahed's adaptive FLC in terms of: transient parameters, steady-state parameters. Here peak overshoot for "proposed controller" is higher than the reference controller but settling time is less than the proposed controller.

Table 4-10 Performance comparison for pitch angle response

Controller	Rise time	Settling time	Peak overshoot	Steady-state error
Proposed Controller	2.8s	11s	20%	0
Adaptive FLC [38]	3.6s	22s	9.43%	0.003

Table 4-11 Performance comparison for yaw angle response

Controller	Rise time	Settling time	Peak overshoot	Steady-state error
Proposed Controller	2.5s	18s	29%	0
Adaptive FLC [38]	2.24s	21s	33.24%	0.0005

Juang et.al. [99] proposed a hybrid Fuzzy PID controller employing real-valued GA for performance optimization.

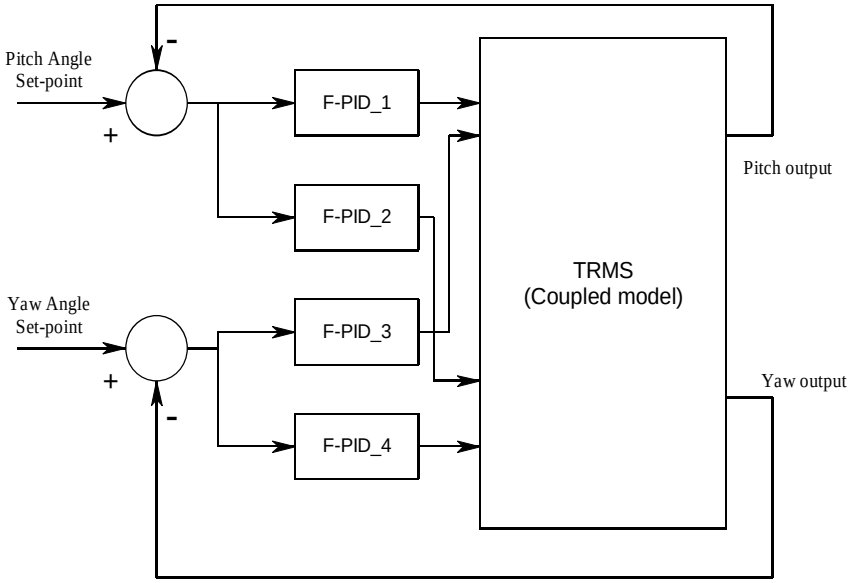

Figure 4-18 Architecture of hybrid Fuzzy-PID controller for coupled TRMS **[99]**

Juang uses coupled characteristics of TRMS, thereby employing 4 hybrid fuzzy-PID controllers, architecture of illustrated in Figure 4-18. The hybrid controller gain is optimized using GA. Following equation represents the system performance index:

$$I_{PITSE} = T^2\left(\int_{t_1}^{t_2}(y(t)-1.1r(t))dt + 2\int_{t_3}^{t_4}(y(t)-1.5r(t))dt + \int_0^{t_r}0.9r(t)dt + \int_{t_{ss}}^{\tau}|y(t)-r(t)|dt + \int_0^{\tau}u^2(t)dt\right) \quad (4\text{-}10)$$

here t_1 and t_3 are the times when $y(t)$ first reaches $1.1r(t)$ and $1.5r(t)$, respectively, and t_2 and t_4 are the second times when $y(t)$ reaches $1.1r(t)$ and $1.5r(t)$, respectively; t_r is the rise time; t_{ss} is steady-state time; M_p is peak overshoot for $y(t)$; where T is system running time. The fitness function utilized is given by:

$$F = \frac{A}{I_{PITSE}} \tag{4-11}$$

here A is a large positive constant.

Figure 4-19 illustrates the comparison for pitch angle response with (a) proposed controller with (b) reference hybrid fuzzy PID controller.

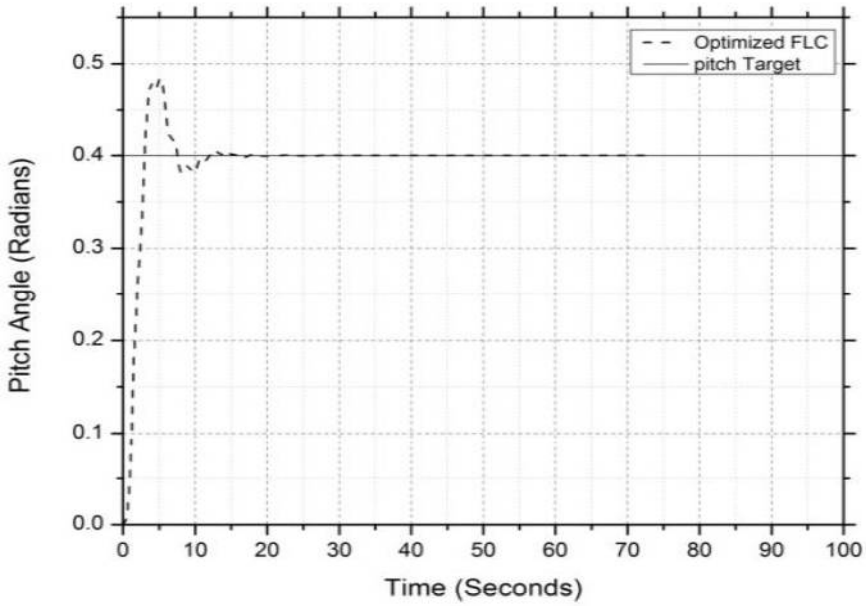

(a)

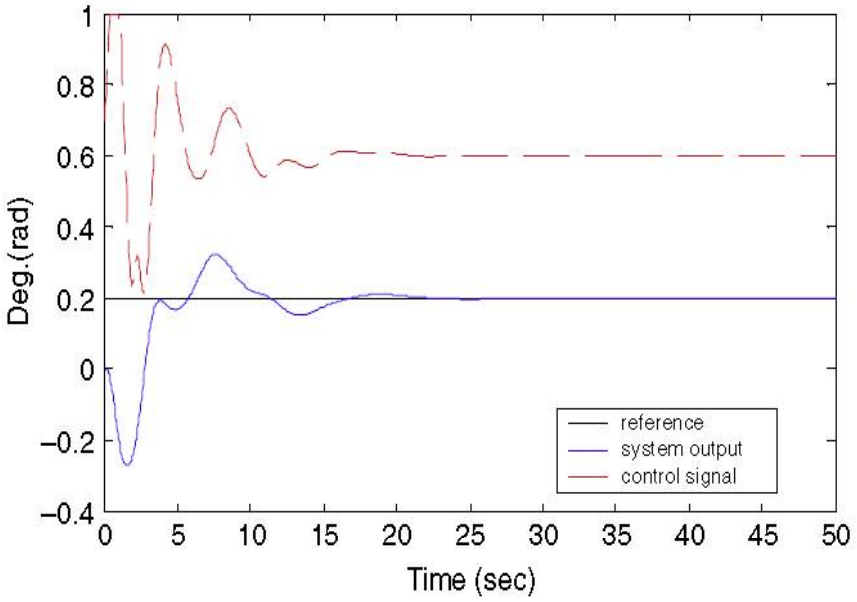

(b)

Figure 4-19 Pitch angle set-point tacking response (a) proposed controller (b) reference controller [99]

Similarly Figure 4-20 depicts the comparison of set point tracking for yaw angle.

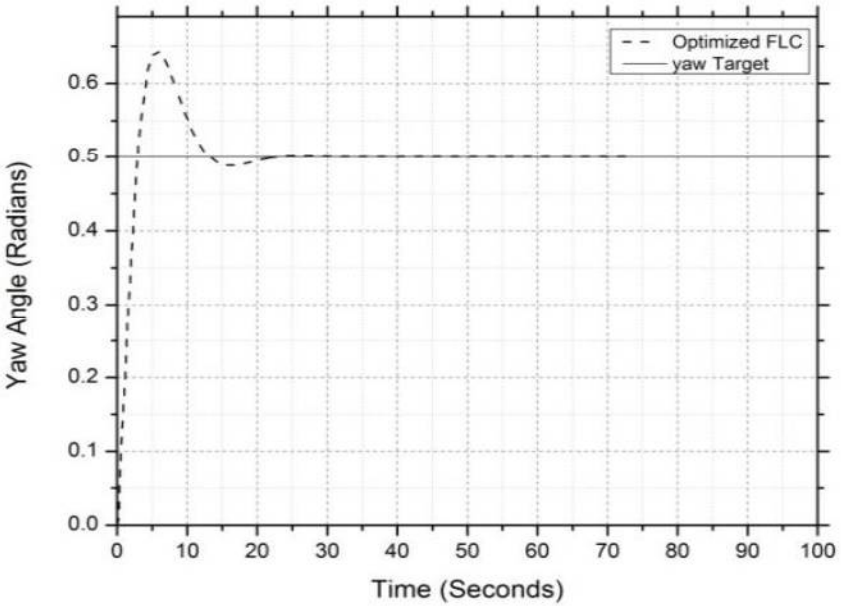

(a)

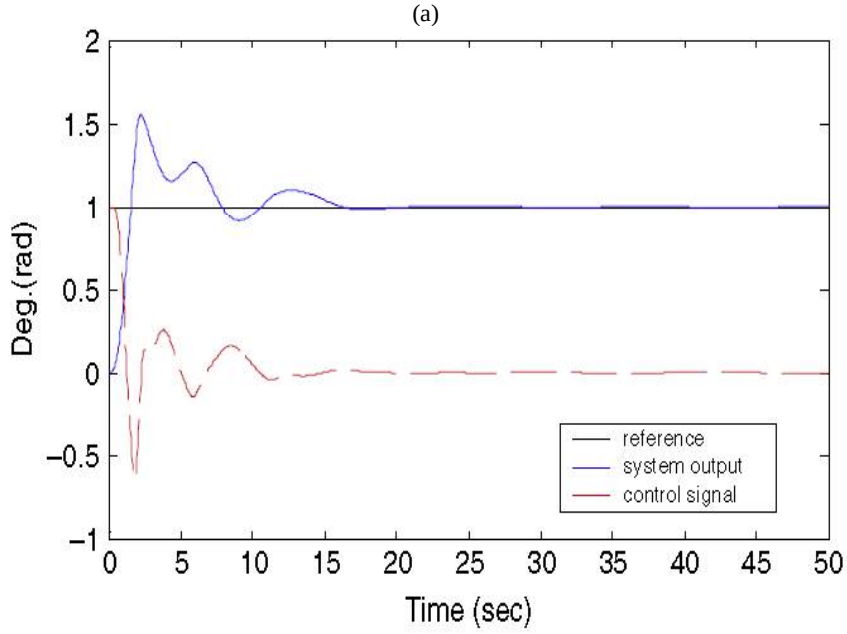

(b)

Figure 4-20 Yaw angle set-point tacking response (a) proposed controller (b) reference controller [99]

Table 4-12 illustrates the comparison for pitch angle response to proposed controller and Juang's hybrid Fuzzy-PID controller in terms of: transient parameters, steady-state parameters. Table 4-13 illustrates the comparison between yaw angle response for proposed controller and Juang's hybrid

Fuzzy-PID controller in terms of: transient parameters, steady-state parameters.

Table 4-12 Performance comparison for pitch angle response

Controller	Rise time	Settling time	Peak overshoot	Steady-state error
Proposed Controller	2.8s	11s	20%	0
Hybrid Fuzzy [99]	4.2s	18s	62%	0

Table 4-13 Performance comparison for yaw angle response

Controller	Rise time	Settling time	Peak overshoot	Steady-state error
Proposed Controller	2.5s	18s	29%	0
Hybrid Fuzzy [99]	2.2s	14s	63%	0.0005

4. 9 Conclusion

This chapter focuses on real-time control of TRMS. Results for the proposed controller are compared with benchmark PID controller, FLC (non-optimized) and reference controllers the obtained results indicate improvement controller performance.

Figure 4-21 illustrates the comparison for pitch angle response with proposed controller with reference controllers for: (a) rise time and (b) settling time. The controllers referenced here are: adaptive FLC design by Jahed [38] and hybrid fuzzy PID controller designed by Juang [99] discussed in section 4. 8. 1.

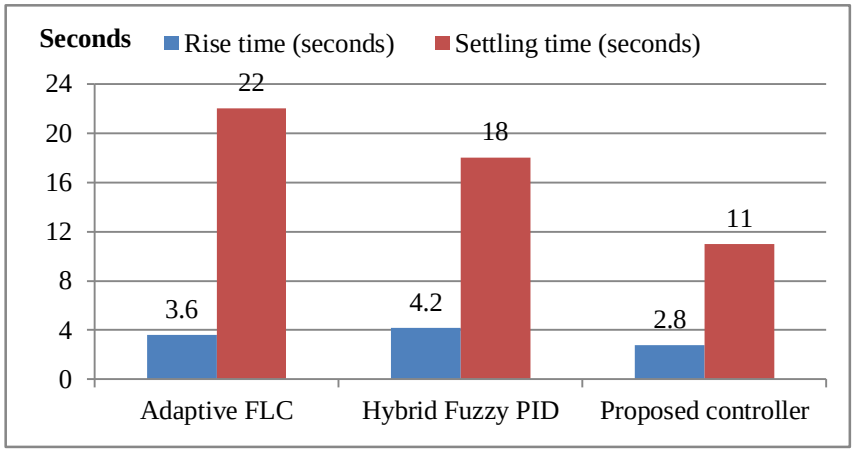

Figure 4-21 Rise time and settling time comparison of proposed controller with reference controllers for pitch angle response

Figure 4-22 illustrates the response comparison for pitch angle for proposed controller with reference controllers for peak overshoot. The controllers referenced here are: adaptive FLC design by Jahed [38] and hybrid fuzzy PID controller designed by Juang [99] discussed in section 4. 8. 1.

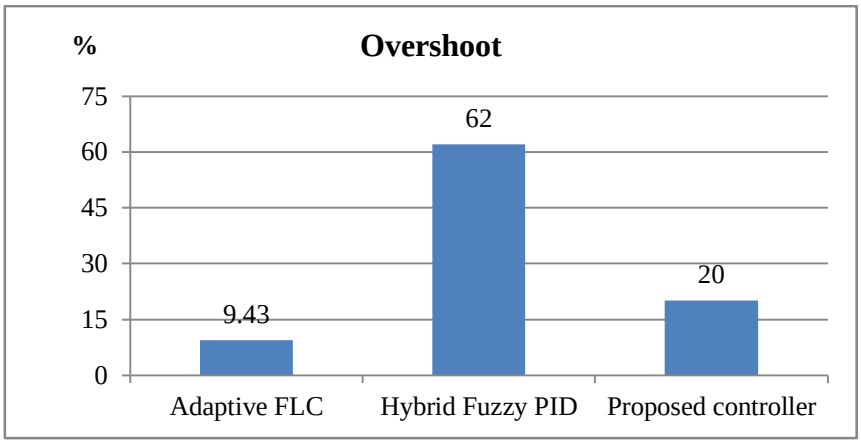

Figure 4-22 Peak overshoot comparison of proposed controller with reference controllers of pitch angle response

Comparison for pitch angle response indicates that proposed controller shows an overall improvement in set-point tracking. The proposed controller exhibits a rise time of 2.8 seconds which is about 22.22% faster than adaptive FLC design by Jahed [38] and 33.33% faster than hybrid fuzzy PID controller designed by Juang [99]. The settling time for proposed controller is 11 seconds which is about 50% faster than adaptive FLC design by Jahed [38] and 38.88% faster than hybrid fuzzy PID controller designed by Juang [99]. The peak overshoot exhibited for proposed controller is 20% which is 10.57% higher than adaptive FLC design by Jahed [38] but is 42% less as compared with hybrid fuzzy PID controller designed by Juang [99].

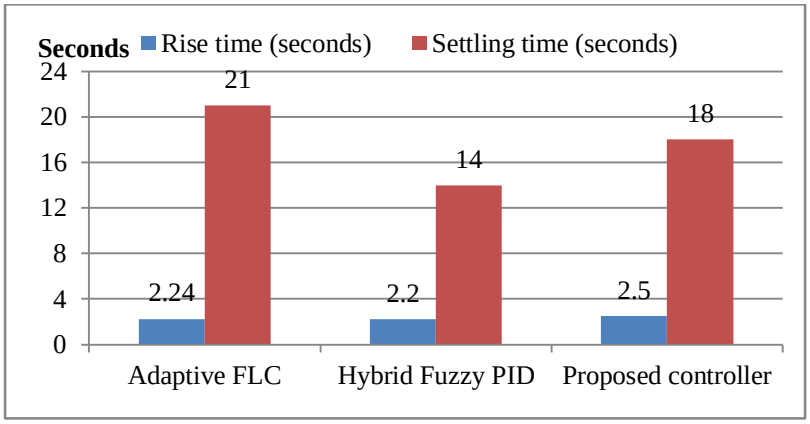

Figure 4-23 Rise time and settling time comparison of proposed controller with reference controllers for yaw angle response

Figure 4-23 illustrates response comparison for yaw angle for proposed controller with reference controllers for: (a) rise time and (b) settling time. The controllers referenced here are: adaptive FLC design by Jahed [38] and hybrid fuzzy PID controller designed by Juang [99] discussed in section 4. 8. 1.

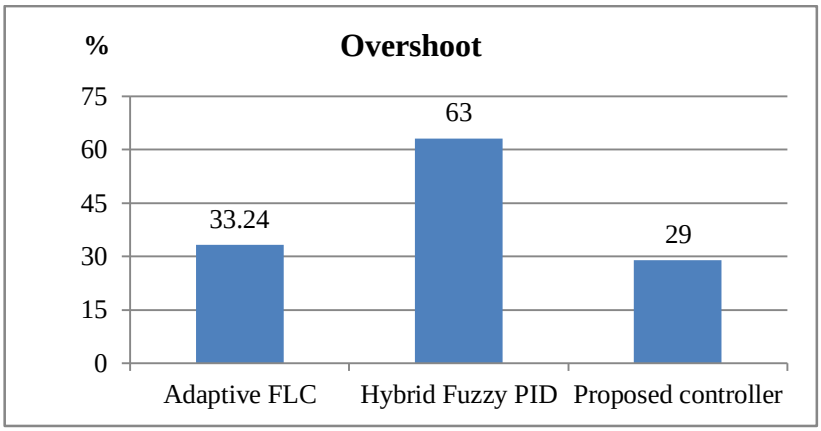

Figure 4-24 Peak overshoot comparison of proposed controller with reference controllers of pitch angle response

Figure 4-24 illustrates response comparison of pitch angle for proposed controller with reference controllers for peak overshoot. The controllers referenced here are: adaptive FLC design by Jahed [38] and hybrid fuzzy PID controller designed by Juang [99] discussed in section 4. 8. 1.

The comparison for yaw angle response indicates that proposed controller shows an overall improvement in set-point tracking. The proposed controller exhibits a rise time of 2.5 seconds which is about 10.4% slower when compared with adaptive FLC design by Jahed [38] and 12% slower than hybrid fuzzy PID controller designed by Juang [99]. Here the referenced controllers' exhibit faster rise-time. However the "settling time" for proposed controller is 18 seconds which is 14.28% faster than adaptive FLC design by Jahed [38] and 22.22% slower than hybrid fuzzy PID controller designed by Juang [99]. Also the peak overshoot for proposed controller is 29% which is 4.24 % less than adaptive FLC design by Jahed [38] and 29% less as compared with hybrid fuzzy PID controller designed by Juang [99].

Reduction in error indices indicates an improvement in response to optimized FLC. For pitch angle set-point tracking the proposed controller exhibits a reduction of about 7.7% in ISE as compared with PID and 1.8% reduction

compared to FLC. The ITSE is reduced by 38.58% as compared with PID and 28.74% as compared with FLC. IAE shows a reduction of 14.94% compared to PID and, reduction of 9.96% as compared with FLC. Similarly ITAE shows a reduction of 42.7% as compared with PID and a reduction of 33.92% as compared with FLC. For yaw angle set-point tracking the proposed controller exhibits a reduction of 32.99% in ISE as compared with PID, reduction of 1.78% compared to FLC. ITSE is now reduced by 51.24% as compared with PID and 4.38% as compared with FLC. IAE shows a reduction of 27.78% as compared with PID and a reduction of 2.96% as compared with FLC. Similarly ITAE shows a reduction of 39.12% as compared with PID and reduction of about 5.96% when compared to FLC. Reduced error indices indicate the steady-state is achieved faster for proposed controller as compared with PID or FLC. Hence an overall improvement of transient and steady-state parameters is observed when compared with PID controller, fuzzy controller and referenced real-time controllers.